minerals

MDPI

Article

Genesis of Precious Metal Mineralization in Intrusions of Ultramafic, Alkaline Rocks and Carbonatites in the North of the Siberian Platform

Anatoly M. Sazonov [1,*], Aleksei E. Romanovsky [1], Igor F. Gertner [2], Elena A. Zvyagina [1], Tatyana S. Krasnova [2], Oleg M. Grinev [2], Sergey A. Silyanov [1] and Yurii V. Kolmakov [3]

[1] Department of Geology, Mineralogy and Petrography, Siberian Federal University, 660041 Krasnoyarsk, Russia; romanovskyi2015@yandex.ru (A.E.R.); elena_zv@mail.ru (E.A.Z.); silyanov-s@mail.ru (S.A.S.)
[2] Department of Geology and Geography, Tomsk State University, 634050 Tomsk, Russia; labspm@ggf.tsu.ru (I.F.G.); science@mail.tsu.ru (T.S.K.); tomskgrom@yandex.ru (O.M.G.)
[3] Department of Geology and Geophysics, Tomsk Polytechnic University, 634050 Tomsk, Russia; kolmakovyv@tpu.ru
* Correspondence: sazonov_am@mail.ru; Tel.: +7-(902)-923-51-77

Abstract: The gold and platinum-group elements (PGE) mineralization of the Guli and Kresty intrusions was formed in the process of polyphase magmatism of the central type during the Permian and Triassic age. It is suggested that native osmium and iridium crystal nuclei were formed in the mantle at earlier high-temperature events of magma generation of the mantle substratum in the interval of 765–545 Ma and were brought by meimechite melts to the area of development of magmatic bodies. The pulsating magmatism of the later phases assisted in particle enlargement. Native gold was crystallized at a temperature of 415–200 °C at the hydrothermal-metasomatic stages of the meimechite, melilite, foidolite and carbonatite magmatism. The association of minerals of precious metals with oily, resinous and asphaltene bitumen testifies to the genetic relation of the mineralization to carbonaceous metasomatism. Identifying the carbonaceous gold and platinoid ore formation associated genetically with the parental formation of ultramafic, alkaline rocks and carbonatites is suggested.

Keywords: carbonaceous-Au-PGM ore formation; ultramafic; alkaline and carbonatite magmatism

Citation: Sazonov, A.M.; Romanovsky, A.E.; Gertner, I.F.; Zvyagina, E.A.; Krasnova, T.S.; Grinev, O.M.; Silyanov, S.A.; Kolmakov, Y.V. Genesis of Precious Metal Mineralization in Intrusions of Ultramafic, Alkaline Rocks and Carbonatites in the North of the Siberian Platform. *Minerals* **2021**, *11*, 354. https://doi.org/10.3390/min11040354

Academic Editor: Martin Smith

Received: 14 January 2021
Accepted: 23 March 2021
Published: 29 March 2021

1. Introduction

Phlogopite, magnetite, chromite, fluorite, apatite, nepheline, diamonds, titanium, uranium, rare and rare earth elements deposits are known in the Maimecha-Kotuy Province associated with intrusions of ultramafic, alkaline rocks and carbonatites. A wide range of minerals associated with this unique magmatism was supplemented in the 1980s with alluvial gold and platinum-group metals (PGM) deposits within the contour of the Guli Intrusion outcrops. To date, no significant hardrock deposits have been discovered in the region. The hardrock gold and platinum mineralization in the Kresty intrusion (satellite of the Guli volcanic–plutonic complex) remains a subject of discussion due to poor reproducibility of the analytical results [1]. The reliability of the presence of platinum-group elements (PGE) and gold in the rocks of the Kresty massif has been confirmed by finds of Au and PGM, confirmed by Wavelength-dispersive spectroscopy (WDS) analyses. No commercial prospecting works for precious metals accompanied by standardized analytics have been carried out within the intrusions, although scientific publications already contain material for geological justification of such works [1–12]. Classifications of noble metal deposits do not contain any data on the formation systematics of gold–platinum deposits in the intrusions of ultramafic, alkaline rocks and carbonatites [2,13]. In this study, we present evidence that the hardrock Au-PGE mineralization in this formation intrusion

in the north of the Siberian Platform was formed during the entire period of occurrence of polyphase magmatism, including the associated hydrothermal and metasomatic stages. The features of formation of ore concentrations within the intrusions suggest the validity of identification of a carboniferous-Au-PGE ore formation.

2. Materials and Methods

The concentrations of PGE, Au and Ag were determined with fire assay methods (40 samples) in the laboratory of the SibtsvetmetNIIproyekt Institute (Krasnoyarsk). The composition of minerals of the PGE and gold from placers of the Gulinskaya area were determined in 286 particles with X-ray microanalysis using a Camebax EPMA in the laboratory of the Geology and Mineralogy Institute of the SB RAS (Novosibirsk, Russia). Scanning electron microscopy of ore minerals from the Kresty Intrusion was carried out using a Tescan Vega II LMU microscope equipped with an energy-dispersive spectrometer with the Si (Li) Standart INCA Energy 350 detector in "Analytical Center for Geochemistry of Natural Systems" (Tomsk). The sensitivity threshold of the fire assay methods is as follows (ppb): for Pt—1.0; Pd—5.0; Rh—0.4; Ir—2.0; Ru—0.4; Os—0.5; Au—0.4; Ag—10.0. Bitumen (malthite, kerite, anthraxolite) were determined in 103 preparations from the rocks of the Kresty intrusion with luminescent microscopy in ultraviolet light. The elementary composition of the non-organic phase from the bitumen chloroform extract was determined with the atomic-absorption method in the Mineralogy Institute of the SB RAS. The Sm and Nd concentrations and their isotope ratios were determined with the method of isotope dilution using the multi-collector mass spectrometer Finnegan MAT-262 (Institute of Geology of Ore Deposits, Petrography, Mineralogy and Geochemistry of the RAS).

3. Results

3.1. Distribution of Au, Ag and PGE in the Rocks of the Guli Intrusion

The multi-phase Guli massif crops out in the form of a half-ring among alkaline volcanics over an area of 470 km^2 (Figure 1). It is the largest of the alkaline-ultramafic intrusions, and it is assumed that about 790 km^2 of the body area is buried under Quaternary deposits of the Yenisei-Khatanga piedmont depression.

Figure 1. (**a**) Geological map of the Guli volcanic–plutonic complex. Compiled based on the materials of L.S. Yegorov and G.G. Lopatin with clarifications and simplifications by O.M. Grinev. 1—Quaternary sediments of the Yenisei-Khatanga piedmont depression; 2—Maimecha Suite (meimechites); 3—subalkaline and alkaline effusives of the Delkan, Kogotok and Arygdjan Suites; 4—complex of deflection alkaline rocks in the intrusive roof; 5—dike complex of the Maimecha Suite (picritic porphyrites); 6—carbonatites (Phase 7); 7—alkaline and nepheline syenites (Phase 5); 8—nephelinites (Phase 4); 9—ijolite-melteigites (Phase 4); 10—melilitic rocks (Phase 2); 11—kosvites (Phase 1); 12—stratified wehrlite–clinopyroxenite complex (Phase 1); 13—dunites and olivinites (Phase 1) 14—hornblende effusives of the roof deflection; 15—fault zones; 16—disjunctives; 17—geological boundaries; 18—placers of the platinum group minerals (**a**) and gold (**b**). (**b**) Geographic position of the Maimecha-Kotuy Province (red contour): G—Guli volcano-pluton; K—Kresty intrusion. r—river.

L.S. Yegorov [14] distinguishes seven phases in the history of formation of the intrusion: olivinite-dunites and pyroxenites (1st), melilitolites (2nd), alkaline ultramafites and gabbroids (3rd), foidolites (4th), nepheline and alkaline syenites (5th), phoscorites (6th) and carbonatites (7th). The photographs of the main rock varieties are provided (Figure 2).

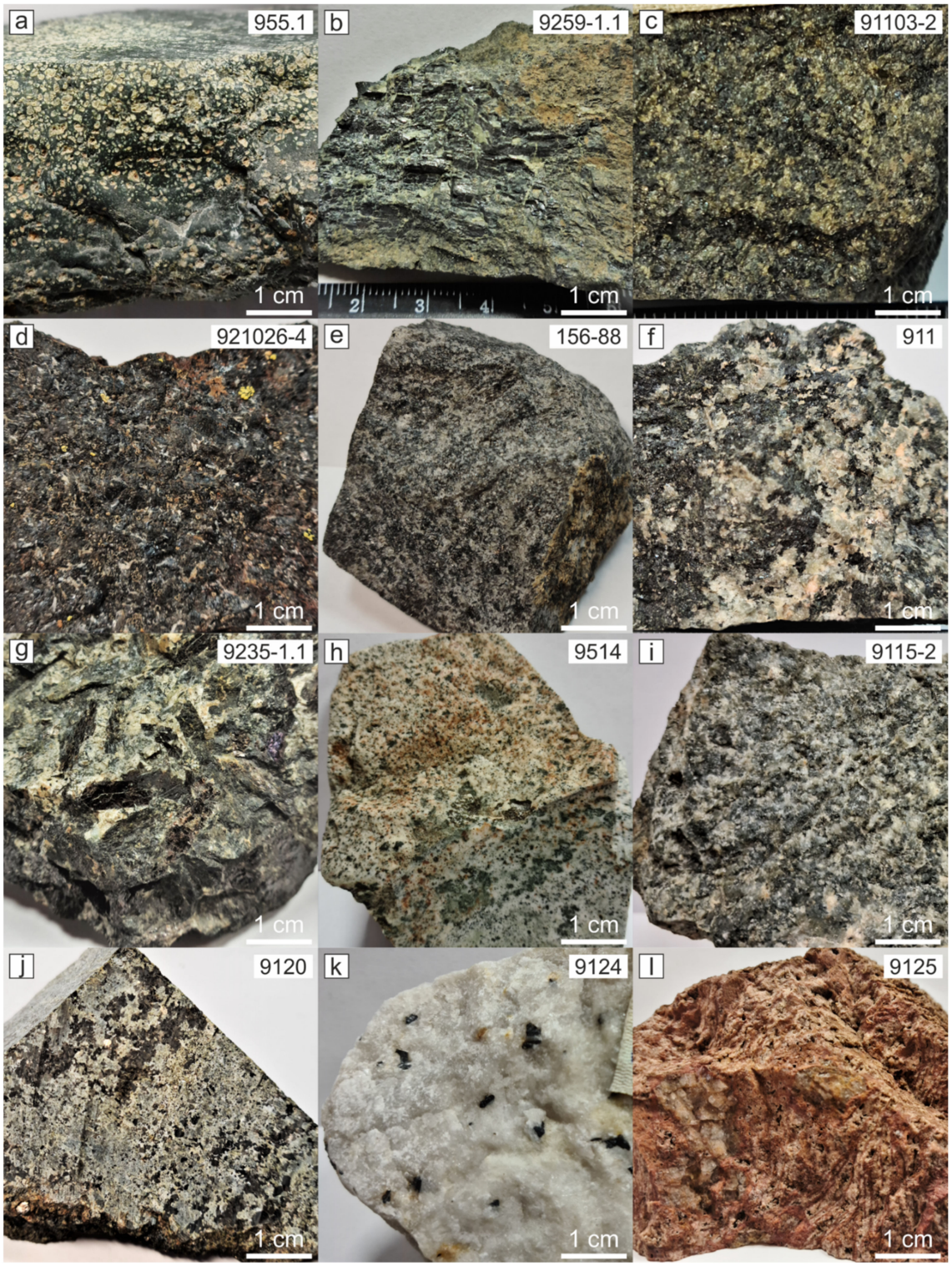

Figure 2. Photographs of the main rock varieties: (**a**) meimechite; (**b**) dunite with chromite schlier; (**c**) ore wehrlite; (**d**) ore pyroxenite; (**e**) kugdite; (**f**) ijolite-melteigite; (**g**) coarse-grained shonkinite; (**h**) alkaline microsyenite; (**i**) foyaite; (**j**) magnetite-apatite-diopside rock; (**k**) calcite carbonatite; (**l**) dolomite carbonatite.

The rock composition of the mass formation phases and the mineral composition of the rocks are given in Table 1.

Table 1. Mineral composition of the rocks of the Maimecha-Kotuy alkaline-ultramafic magmatic complex [14].

Rocks	Main Minerals	Secondary and Accessory Minerals
	Ultramafic Rocks (Phase 1)	
Dunites, olivinites, and ore olivinites, pegmatoid olivinites, ore pyroxenites (kosvites), porphyroid trachitoid olivine pyroxenites	Olivine (Fa—6.2–8.8% in pegmatoids up to 9–11%), monocline pyroxene (augite-diopside), chromite (titanium-ferrichromite), titanium magnetite	Perovskite, apatite, green spinel, phlogopite, clinohumite, serpentine
	Melilite Rocks (Phase 2)	
Melilitolites, uncompagrites, turjaites, okaites, kugdites	Melilite, clinopyroxene, (augite-diopside and diopside, especially in apomelilitic rocks), olivine (Fa—10–15%), nepheline, titanium magnetite	Perovskite, phlogopite, garnet (andradite, grossular), monticellite, cebollite, juanite, calcite, cancrinite, apatite, amphibole, wollastonite, vesuvian, pectolite
	Alkaline Ultramafites and Gabbroids (Phase 3)	
Jacupirangites, melteigites, melanephelinites, malignites, shonkinites	Clinopyroxene (augite-diopside Na_2O > 0.5%), (aegirine-augite), nepheline, titanium magnetite, olivine (Fa—12–18%)	Phlogopite, apatite, titanite, perovskite, natrolite, cancrinite, calcite, anorthoclase, kaersutite, ferro-edenite, zeolites, pyrite, lamprophyllite, fluorite, allanite-(Ce)
	Foidolites (Phase 4)	
Ijolites, ijolite-pegmatites, microijolites	Nepheline, clinopyroxene (aegirine-augite)	Titanium magnetite, phlogopite (ferriferous), cancrinite, calcite, zeolites, apatite, titanite, perovskite, wollastonite, garnet, pyrrhotite
	Nepheline and Alkaline Aegirine Syenites (Phase 5)	
Nepheline syenites, cancrinite-nepheline syenites, alkaline, aegirine syenites, nordmarkites, orthoclase-aplites	Nepheline, anorthoclase, cancrinite, aegirine, aegirine-augite, orthoclase	Apatite, biotite, titanite, zeolites, magnetite, alkaline amphibole (arfvedsonite), albite, pectolite, lamprophyllite, lovchorrite, eudialyte, elpidite, zircon, monazite, quartz
	Phoskorites (Phase 6)	
Diopsidites, forsteritites, phoskorites and apatitic phoskorites, pyroxenitic and apatite-pyroxene nelsonites, olivine nelsonites, nelsonites, apatitites, magnetites	Diopside, aegirine-augite, apatite, magnetite, olivine (Fa—1–5 to 10–20%), forsterite	Phlogopite, richterite, calcite, clinohumite, perovskite, Mg-spinel, monticellite, baddeleyite, pyrochlore, titanite, serpentine, pyrite, pyrrhotite
	Carbonatites (Phase 7)	
Calcitic carbonatites, dolomitic carbonatites	Calcite, dolomite, apatite	Forsterite, magnetite, phlogopite, perovskite, baddeleyite, calcicrete, nepheline, aegirine-augite, melilite

The age of the main magmatism phase is estimated equal to 225 Ma, with the K-Ar dating fluctuation within 375–75 Ma [14]. Table 2 shows data on the age of the rocks of the Guli intrusion, carried out by researchers in different years.

Table 2. Age of the igneous rocks of the Guli volcanic–plutonic complex [15].

Rock/Suite	Mineral	Method	Age, Ma	Reference
Meimechite/Maimecha Suite	Biotite	Ar/Ar	246 ± 1.2	[16]
Meimechite/Delkanskaya Suite	Zircon	U/Pb	251.1 ± 0.3	[17]
Meimechite/Arygdjan Suite	Perovskite	U/Pb	251.7 ± 0.4	[17]
Melanephelinites/Arygdjan Suite (low part)	Bulk Rock	Ar/Ar	253 ± 2.6	[18]
Carbonatites/Guli Complex	Baddeleyite	U/Pb	250.2 ± 0.3	[17]
Bulk Guli Complex	Bulk Rock	U/Pb	250 ± 9.0	[19]
Tuffes/Delkanskaya Suite	Bulk Rock	Pb/Pb (TIMS)	251.9–251.5	[20]
Lavas/Arygdjan Suite	Bulk Rock	Pb/Pb (TIMS)	252.3–252.2	[20]

We have performed analytical studies to determine the precious metals' distribution in the rocks of the Guli intrusion (Table 3; Figure 3). The excess in concentrations, in excess relative to the average crustal concentrations, has been revealed: Pt—in meimechites, dunites, chromitites, magnetitites, melilitolites, nepheline pegmatites; Pd—in all analyzed rock varieties of the intrusion; Rh—in the rocks of Phases 1, 2 and 3; Ir—in the rocks of Phases 1, 2, 3, and 5; Ru—in mylonites of Phase 1, rocks of Phase 3 and skarned melilitolites (Phase 2); Os—in chromitites (Phase 1); Au—in magmatites and metasomatites of all phases except for serpentinite; Ag—in the rocks of all phases except for the rocks of Phase 3, magnetitites and serpentinites. The concentrations of elements are commonly lower than in chondrite (C-1), except for silver in almost all rocks and palladium in phlogopite porphyrite (Phase 3), agpaitic nepheline syenite (Phase 5) and mylonite of dunite.

Table 3. Concentrations of precious metals in the rocks of the Guli intrusion, ppb.

Item No.	Rock	Pt	Pd	Rh	Ir	Ru	Os	Au	Ag
1	Meimechite (n = 2) *	29	179	6.3	5.1	<0.4	1.8	43	300
2	Dunite (n = 3)	24	159	6.1	2.6	<0.4	22.2	24	247
3	Chromitite with magnetite (n = 7)	21	148	2.3	56.4	6.6	58.6	23	12
4	Ore pyroxenite (n = 9)	50	256	5.7	7.9	2.6	6.7	36	362
5	Magnetitolite (n = 2)	83	305	15	7.0	1.1	3.0	79	n.d.
6	Serpentinite (n = 1)	<1	13.6	<0.4	<2.0	1.2	3.2	<0.4	<10
7	Serpophite-magnetite rock (n = 3)	<1	155	<0.4	<2.0	4.4	n.d.	14	<10
8	Melilitolite (n = 2)	36	209	8.0	7.4	7.1	3.5	96	74
9	Phlogopite porphyrite	<1	1890	9.5	10.0	18.8	n.d.	26.7	<10
10	Melilite-magnetite skarn	37	248	9.0	5.8	14.0	7.0	143	220
11	Mylonite of dunite	592	1790	654	22.0	38.8	8.1	15.6	150
12	Ijolite (n = 3)	<1	79	<0.4	<2.0	<0.4	6.7	20	364
13	Nepheline pegmatite (n = 5)	6.5	657	<0.4	2.5	0.4	1.0	32	396
14	Agpaite nepheline syenite (n = 3)	<1	1748	<0.4	<2.0	<0.4	5.0	0.8	125
15	Foyaite (n = 3)	n.d.	<5	<0.4	2.0	<0.4	14.0	0.7	107
16	Calcite carbonatite (n = 3)	<1	451	0.7	<2.0	0.4	0.6	6.2	225
17	Dolomite carbonatite (n = 3)	<1	703	1.0	<2.0	<0.4	n.d.	210	300

* (n = 2)—number of analyses; n.d.—not detected.

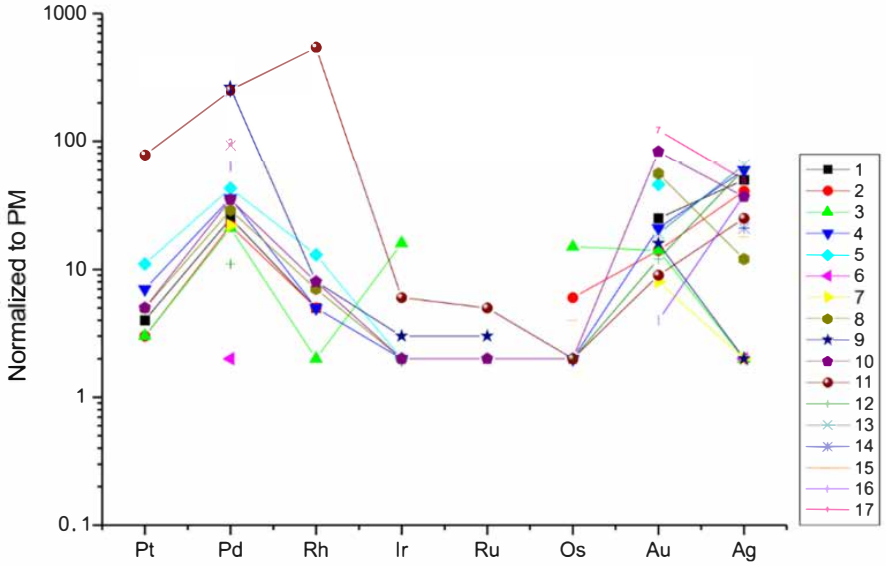

Figure 3. Primitive mantle-normalized [21] spidergram of the platinum-group elements (PGE), Ag and Au content in the rocks of the Guli Intrusion (for the description of the numbers, see Table 3).

The maximum content of PGE (mainly due to palladium) in the rocks of the differentiated complex was identified in phlogopite porphyrites (1.9 ppm), agpaitic nepheline

syenites (1.76 ppm) and dynamometamorphites of dunites and peridotites (3.1 ppm). The highest gold grades were recorded in melilitolites and their skarned varieties, magnetitolites and dolomite carbonatites.

Thus, igneous rocks of Phases 1, 2, 3, 5 and 7, and the associated alkaline and mafic metasomatites, take part in the formation of geochemical anomalies of precious metals. Dunite, among the chromite aggregates, also contains particles of the Ru-Os-Ir composition in an aggregate with chalcopyrite and Ru-Os-Ir sulfide (Figure 4a). Dunite olivine contains aggregates of djerfisherite ($K_6(Fe,Cu,Ni)_{25}S_{26}Cl$) with talnakhite and chalcopyrite with bornite (Figure 4b).

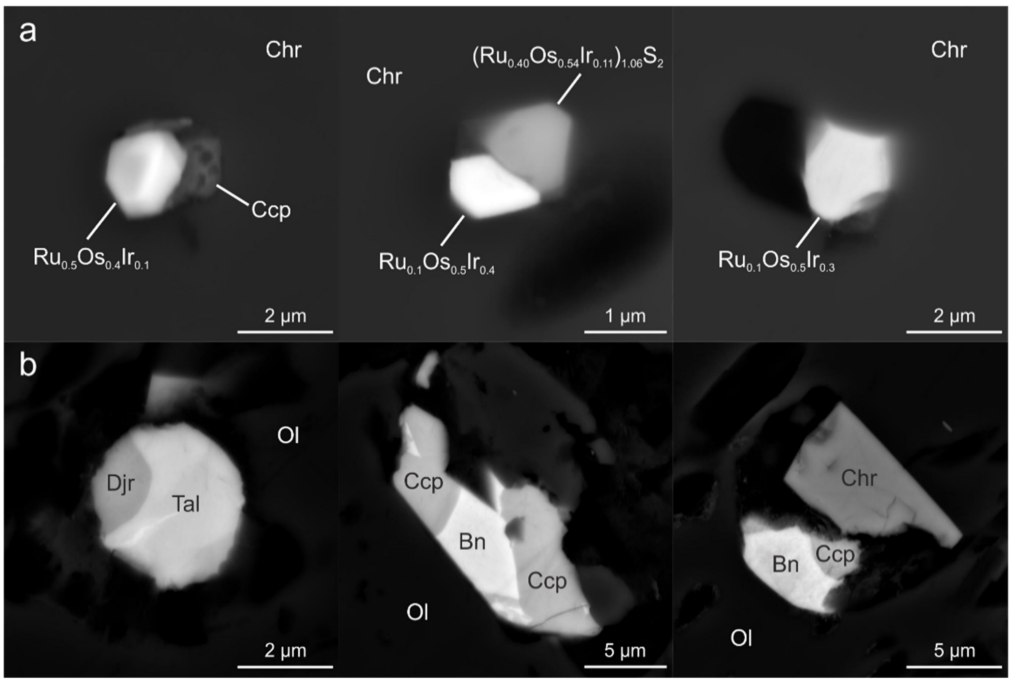

Figure 4. Backscattered-Electron (BSE) photographs of the platinum-group metals (PGM) (**a**) and sulfides (**b**) in dunites. Ccp—chalcopyrite; Chr—chromite; Ol—olivine; Djr—djerfisherite ($K_6(Fe;Cu;Ni)_{25}S_{26}Cl$); Tal—talnakhite ($Cu_9(Fe;Ni)_8S_{16}$); Bn—bornite ($Cu_5FeS_4$).

3.2. Alluvival Mineral Associations of the Guli Intrusion

Minerals of the precious-metal complex, discovered in placers within the Guli intrusion, are represented by native osmium and gold (Figures 5 and 6). Isoferroplatinum (Pt_3Fe) and palladic ferroplatinum (Pt,Fe) are subordinated and form pockets in osmium aggregates. Refractory PGM sulfoarsenides (erlichmanite OsS_2, laurite RuS_2, tolovkite IrSbS and irarsite (Ir,Ru,Rh,Pt)AsS) are found in the form of fine accretions in native osmium aggregates.

The compositions of the platinum metal minerals are given in Figure 7.

According to the mining data, in the placer of the Gule River, about 10% of the platinum pan sample contained euhedral native osmium monocrystals, the size of the latter being over 2.0 mm. Findings of precious metal minerals in the bedrock occurrence are extremely rare. Isoferroplatinum and palladic ferroplatinum form microscopic pockets in native osmium aggregates. Refractory PGM sulfoarsenides (erlichmanite, laurite, tolovkite and irarsite) are found in the form of fine accretions in native osmium crystals. Iron, nickel and copper sulfides are found with them. The paragenetic interrelations between the noble metal minerals are illustrated in Figure 8.

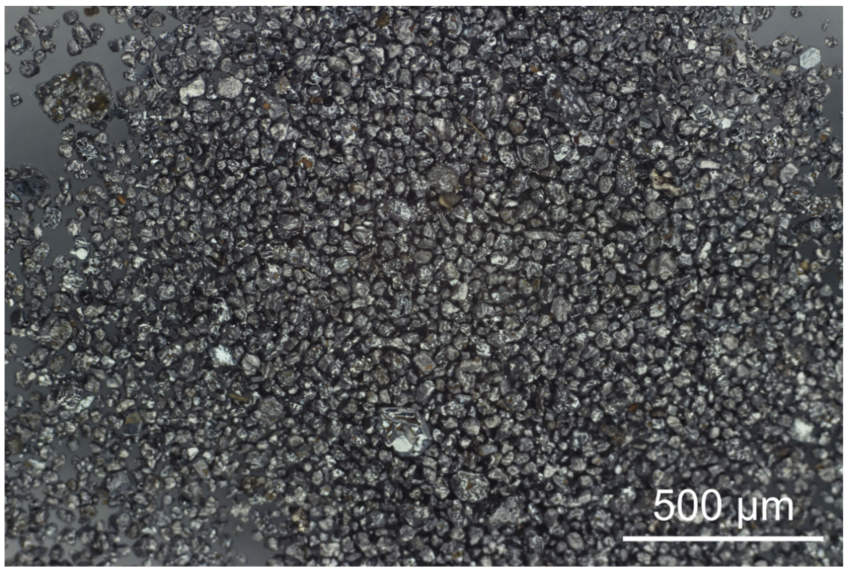

Figure 5. PGM concentrate from the Gule River placer (photo by B. Lobastov).

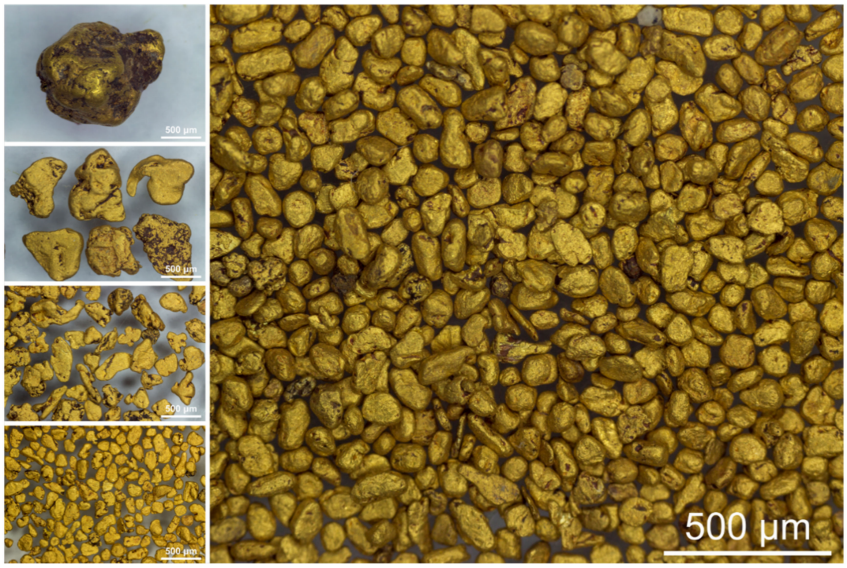

Figure 6. Native gold concentrate from the Gule River placer (photo by B. Lobastov).

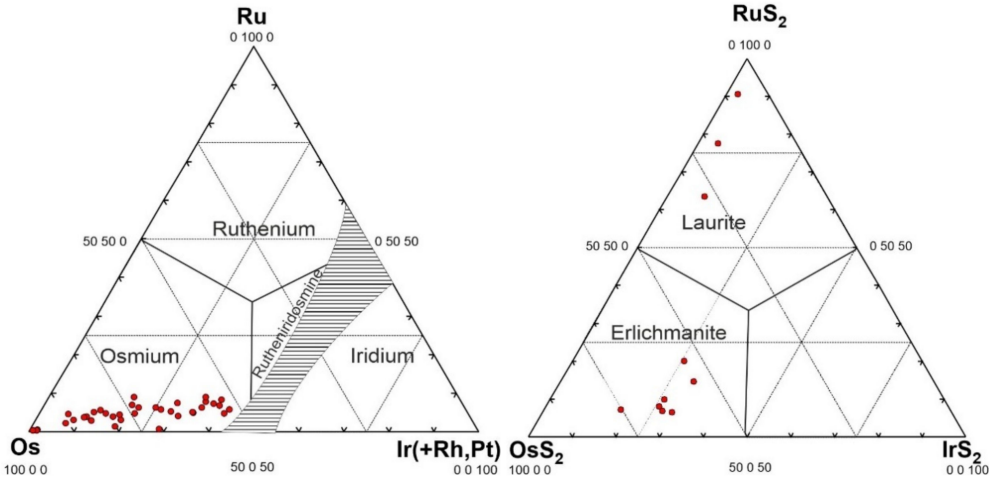

Figure 7. Ternary plots depicting the compositions of the platinum group minerals.

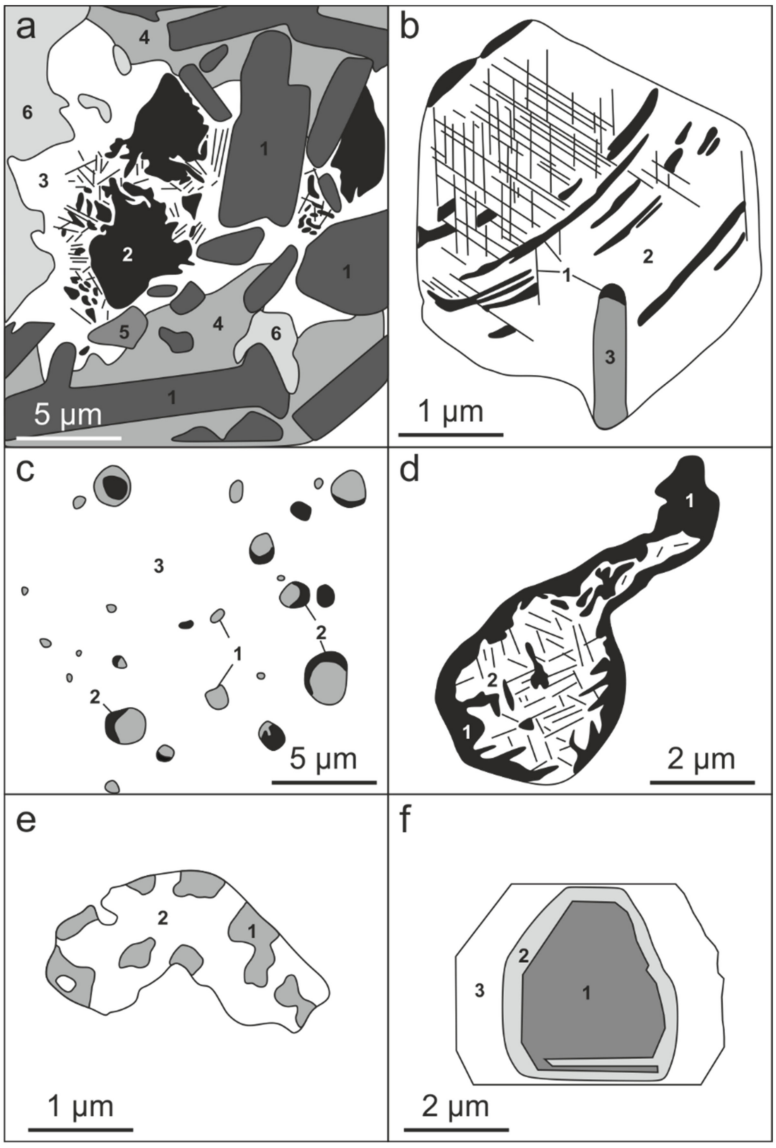

Figure 8. Types of mineral aggregates of the PGM and gold: (**a**) nature of the interrelations of native osmium (1), osmiridium (2), irarsite (Ir,Ru,Rh,Pt)AsS (3), isoferroplatinum Pt_3Fe (4), erlichmanite OsS_2 and tolovkite IrSbS (5), and silicates (6) in a polymineral aggregate; (**b**) Pt-Ir-Ru alloy isostructural ingrowths (1) in isoferroplatinum (2) containing relic native iridium (3); (**c**) two-phase inclusions of erlichmanite (1) and pyrrhotite (2) in native iridium (3); (**d**) decomposition structures of cuproaurite (1) and gold (2); (**e**) polygonal phases of gold (1) and electrum (2); (**f**) native osmium (Os_{98}) crystal (1) with increasing zones of the mineral with variable composition: $Os_{54}Ir_{39}Ru_5$ (2) an $Os_{67}Ir_{33}$ (3). The figures are based on photographs.

Native gold was studied in gold-bearing bedrock crushed samples and prospecting working pan samples along the Selingde, Vetvistaya, Ingaringda, Vostochnaya, Pois-kovaya and Gule Rivers. Native gold particle sizes predominate in the less than 2 mm fraction. About 5% of the metal was recorded in some cases in the 1–2 cm fraction. The roundness of the particles increases with their size. Variability in the color of the particles from white to various intensities of yellow and red is typical. The majority of particles have a gold–silver composition corresponding to three chemical types of the mineral (Au wt. %: 61.1–68.6, 76.1–83.6 and 91.0–98.5). Particles of the last two fineness classes are the most widespread. Some compositions of the mineral are characterized by a notable Cu content. Composition points within the diagram are grouped along the line parallel to the solvus isotherm of the Au-Ag-Cu system for a temperature below 400 °C (Figure 9). Several determinations of the

mineral composition correspond to cuproaurite. Emulsive, parallel-plate and lattice-like couproaurite aggregates were observed in gold from samples 833, 750 and in electrum (650‰, 636‰ and 575‰). Sometimes cuproaurite forms a continuous margin around electrum. In this case, worm-like ingrowths of electrum are observed in cuproaurite, and lattice-like aggregates of cuproaurite are observed in the inner zone of the electrum (Figure 8d). Iron, zinc, lead, arsenic, antimony, tellurium and mercury were measured in gold minerals with concentrations typically ranging from 0.05 to a tenth %.

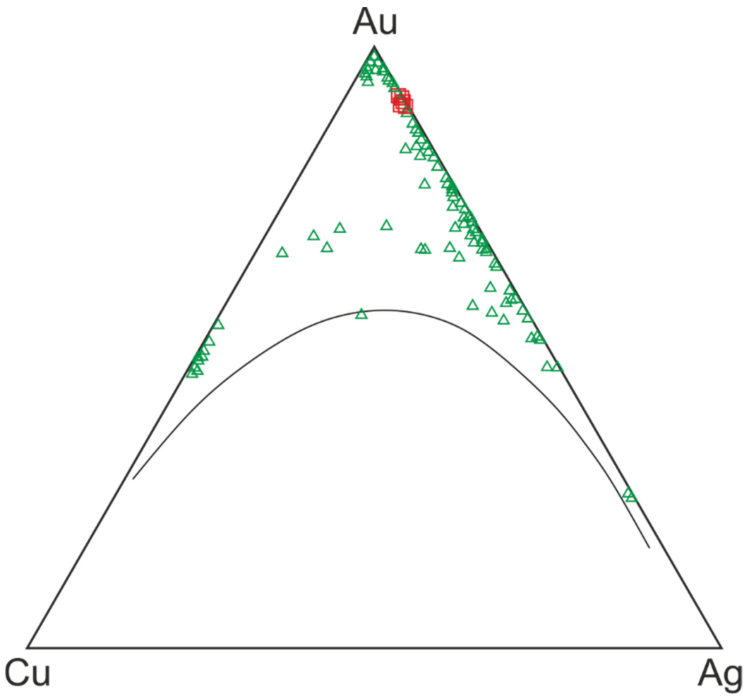

Figure 9. Composition of placer gold from the placer of the Gule River (green triangles) and bedrock gold particles from olivine rocks (red squares) [11].

Widespread barren rock-forming minerals entrapped in native osmium, iridium and gold bear important genetic information [1,6]. Optically detected and electron-microscopically confirmed entrapped minerals are forsterite and Fe-rich olivine, serpentines, diopsides, magnesian-ferriferous mica of the phlogopite-biotite series, pargasite, titanite, silicate glass, chromite, chrome-magnetite, ishkulite ($Fe(Fe,Cr)_2O_4$) and ilmenite (Tables 4 and 5).

These minerals are the main rock-forming minerals of the corresponding rocks of the polyphase intrusion. Paragenetic associations of the host minerals of the platinum metals and gold with magmatic and entrapped hydrothermal rock-forming minerals allow inferring their formation and repeated recrystallization due to the polyphase magmatic-hydrothermal processes of the massif formation. The most reliably established parageneses of the host minerals and entrapped minerals allow making the following conclusions about the time of crystallization and transformation of mineral aggregates of platinum metals (Tables 1 and 4).

1. The association: native osmium + forsterite + chromite, judging by the presence of forsterite and chromite in it, was formed during the first phase of magmatism in the course of crystallization of olivine rocks and pyroxenites.
2. The association: native ir-osmium ± hyalosiderite ± aegirine-diopside ± aegirine-augite ± phlogopite corresponds to the fourth phase, the formation of foidolites, in terms of the set of barren minerals.

3. The association: native osmium ± isoferroplatinum ± ir-osmium ± irarsite + aegirine ± ilmenite ± alkali feldspars ± erlichmanite ± chalcopyrite corresponds to the fifth phase of magmatism, the formation of nepheline and alkaline syenite bodies.

Table 4. Chemical composition of the minerals entrapped in native osmium, wt. %.

Item No.	Place of Sampling (Watercourse)	Sample No.	Entrapped Mineral	SiO_2	TiO_2	Al_2O_3	Cr_2O_3	MnO	FeO	MgO	CaO	Na_2O	K_2O	Sum
1	Gule	A3	chrysolite	38.96	0.00	0.00	0.04	0.40	15.04	43.34	0.18	0.00	0.00	98.40
2	Gule	A4	forsterite	40.70	0.03	0.05	0.00	0.29	7.79	49.01	0.21	0.00	0.00	98.28
3		A6		40.45	0.00	0.01	0.00	0.22	8.98	47.70	0.43	0.00	0.00	98.16
4	Gule	A4/1	hyalosiderite	36.57	0.05	0.31	0.02	0.72	29.62	30.81	0.08	0.11	0.00	98.34
5		B15		36.50	0.11	0.00	0.00	0.52	27.62	33.52	0.10	0.00	0.00	98.52
6	Gule	A4/1	augite-diopside	52.19	0.94	0.86	0.09	0.08	4.96	14.28	22.90	1.09	0.00	97.39
7		A4/2		52.34	0.70	0.86	0.02	0.25	5.64	13.92	23.19	1.22	0.00	98.14
8		B15		52.42	1.09	0.91	0.07	0.18	4.90	14.46	22.90	0.85	0.00	97.78
9	Dunitovy	P-21		49.55	1.16	2.80	0.01	0.07	8.06	12.15	20.97	1.57	0.09	96.42
10	Dunitovy	B15	aegirine-augite	43.99	3.99	8.07	0.24	0.02	7.42	15.76	10.71	3.79	0.37	94.40
11		B33		52.61	0.27	1.79	0.04	0.17	5.40	22.14	9.79	2.13	0.00	94.95
12		P-21		43.91	4.25	7.01	0.06	0.09	12.00	11.48	16.12	2.90	0.63	98.47
13		P-21		43.27	3.68	8.22	0.08	0.07	11.43	11.52	13.12	3.17	0.66	95.21
14	Vostochny	A4/2	aegirine	48.22	1.08	4.56	0.03	0.15	10.46	15.62	7.48	6.12	0.19	94.72
15		B33		49.27	0.23	10.16	0.09	0.11	6.84	8.84	14.68	6.02	1.12	97.61
16	Vostochny	A3/1	phlogopite	40.40	1.27	12.04	0.08	0.05	6.05	24.22	0.09	1.46	7.94	93.78
17		A4/1		39.88	1.70	12.14	0.08	0.03	7.88	21.73	0.13	2.33	6.94	92.53
18		A4/2		36.14	3.10	12.03	0.20	0.14	13.55	15.82	0.08	1.03	8.24	90.49
19		B15		31.87	3.32	10.25	1.08	0.07	6.45	12.07	0.29	0.99	6.70	73.19
20	Vostochny	A4/1	phase not diagnosed	40.86	0.90	7.90	2.99	0.03	6.94	19.14	6.72	2.20	4.33	92.01
21		P-8		40.14	4.00	24.73	0.07	0.09	10.00	4.53	0.31	6.32	9.12	99.30
22	Dunitovy	P-21	chromite	0.08	4.51	3.34	30.88	0.41	50.62	5.79	0.02	0.22	0.02	96.20
23		P-21		0.02	3.76	3.89	30.79	0.35	52.22	6.36	0.02	0.15	0.00	97.54
24		A6		bdl	1.87	12.16	41.45	0.56	34.55	8.35	bdl	bdl	bdl	99.24
25		N6		bdl	1.92	11.95	40.33	0.48	30.04	8.02	bdl	bdl	bdl	99.26
26		A10		bdl	1.88	11.91	39.84	0.47	35.55	8.29	bdl	bdl	bdl	98.10
27		A10		bdl	1.93	12.36	41.56	0.47	34.46	8.07	bdl	bdl	bdl	99.01
28		A25		bdl	3.57	6.34	45.49	0.27	34.81	9.30	bdl	bdl	bdl	100.05
29		A25		bdl	4.62	6.25	46.17	0.29	34.78	9.49	bdl	bdl	bdl	101.68
30	Dunitovy	A5	magnetite	bdl	0.00	0.03	0.00	0.96	95.40	0.54	bdl	bdl	bdl	96.63
31		A5		bdl	0.11	0.00	0.00	1.58	93.94	0.83	bdl	bdl	bdl	96.46
32	Gule	P-8	ilmenite	0.09	36.81	1.55	1.24	0.39	49.99	9.84	0.07	0.20	0.02	100.23

bdl—below detection limit.

Table 5. Chemical composition of the minerals entrapped in gold, wt. %.

Item No.	Place of Sampling (Watercourse)	Sample No.	Entrapped Mineral	SiO_2	TiO_2	Al_2O_3	Cr_2O_3	MnO	FeO	MgO	CaO	Na_2O	K_2O	Sum
1	Gule	A-17	olivine	40.70	0.01	0.00	0.01	0.06	7.46	49.10	0.23	0.01	0.00	97.66
2		A-2		38.68	0.08	0.61	0.03	0.07	9.03	36.74	0.22	0.08	0.01	85.55
3	Poiskovy	A-48	diopside	52.53	0.00	2.15	0.29	0.24	2.29	15.73	24.32	0.37	0.03	97.91
4		unnumb.		52.26	0.00	2.25	0.15	0.38	2.90	15.21	23.93	0.39	0.11	97.59
5	Vetvisty	A-69	augite-diopside	53.31	0.08	1.02	0.00	0.17	5.84	13.41	23.68	0.50	0.00	98.02
6		A-69		51.84	0.19	1.08	0.00	0.30	7.48	13.55	24.16	0.76	0.02	99.39
7	Khanar	A-70		44.06	2.98	2.04	1.24	0.07	9.47	14.33	20.08	0.83	0.00	95.11
8	Gule	A-17		48.63	2.38	2.58	0.00	0.11	8.57	15.10	21.75	0.38	0.02	99.52
9		A-27		50.43	1.12	2.77	0.15	0.19	11.14	14.99	19.69	0.28	0.01	101.07
10	Poiskovy	A-48		44.64	4.15	4.63	0.01	0.06	7.94	13.29	21.83	0.87	0.09	97.50
11	Dunitovy	A-46		48.88	3.24	2.95	0.04	0.06	5.81	15.45	22.76	0.70	0.06	99.95
12	Gule	A-8	aegirine-augite	54.74	0.14	0.97	0.06	0.04	1.91	23.60	12.03	3.21	0.07	96.72
13		A-8		56.62	0.06	0.90	0.02	0.01	1.13	23.11	10.60	3.18	0.06	95.70
14	Dunitovy	unnumb.		48.21	0.62	4.83	0.00	0.33	14.17	14.25	10.60	4.33	0.11	97.43
15		unnumb.		46.79	0.48	6.32	0.01	0.25	15.15	14.54	10.22	4.89	0.13	98.76

Table 5. *Cont.*

Item No.	Place of Sampling (Watercourse)	Sample No.	Entrapped Mineral	SiO_2	TiO_2	Al_2O_3	Cr_2O_3	MnO	FeO	MgO	CaO	Na_2O	K_2O	Sum
16	Gule	A-25	aegirine	52.75	1.12	0.73	0.23	0.02	25.34	1.47	1.23	13.76	0.00	96.66
17		A-25		52.57	0.35	0.24	0.04	0.06	24.56	2.53	6.18	10.25	0.00	96.79
18		A-25		53.56	1.02	0.84	0.43	0.02	25.07	1.45	1.22	12.88	0.01	96.49
19		A-33		50.73	1.71	3.05	0.36	0.03	14.68	13.59	0.37	10.48	0.29	95.31
20	Maimecha	A-71		50.55	2.10	1.11	0.05	0.01	28.05	1.37	0.69	14.77	0.04	96.75
21		A-71		51.97	1.35	1.19	0.08	0.01	25.60	1.40	0.53	13.30	0.03	95.47
22	Gule	A-21	arfvedsonite	48.64	0.24	2.69	0.42	0.08	12.32	17.44	1.62	6.69	0.30	90.72
23		A-33		48.13	1.53	2.64	0.20	0.04	15.14	11.72	0.29	9.69	0.28	89.65
24		A-33		50.86	0.40	1.78	0.06	0.03	14.40	14.80	1.03	9.55	0.26	93.15
25	Dunitovy	A-44		47.73	0.41	1.35	0.03	0.17	18.80	10.12	2.94	7.02	0.07	88.64
26	Gule	A-26	albite	68.87	0.02	20.44	0.01	0.01	0.27	0.17	0.19	9.93	0.89	100.80
27	Maimecha	A-27	albite	57.96	0.16	19.22	0.07	0.03	3.07	0.46	1.55	10.13	0.56	93.21
28	Gule	A-25		68.16	0.00	19.88	0.19	0.00	0.05	0.01	0.01	10.19	0.00	98.48
29		A-25		66.77	0.01	19.75	0.46	0.01	0.14	0.02	0.09	7.72	0.04	95.01
30	Maimecha	A-71	nepheline	32.51	0.01	29.76	0.06	0.02	0.03	0.02	0.01	17.90	0.00	80.31
31		A-71		34.67	0.00	31.21	0.03	0.00	0.02	0.00	0.00	16.89	0.00	82.82
32	Gule	A-32	garnet	36.28	1.15	7.13	0.00	0.26	19.58	0.22	32.48	0.19	0.02	97.30
33		A-15		38.70	2.22	12.70	0.11	0.02	5.28	4.26	28.71	0.04	0.10	92.15
34		A-18	titanite	34.92	30.63	1.13	0.01	0.02	4.36	4.31	23.55	2.17	0.31	101.13
35		A-18		31.75	34.62	0.33	0.02	0.00	1.01	0.81	27.23	0.38	0.00	96.15
36		A-18		32.09	33.06	0.46	0.01	0.00	1.52	1.44	26.33	0.73	0.01	95.66
37		A-25		29.22	42.15	0.01	0.00	0.00	0.16	0.04	27.06	0.89	0.00	99.53
38		A-38		29.36	39.86	0.20	0.00	0.00	0.93	0.05	28.10	0.17	0.01	98.66
39	Dunitovy	A-40		29.45	41.09	0.07	0.00	0.01	0.36	0.04	27.53	0.45	0.00	99.01
40		A-47		30.13	39.55	0.25	0.00	0.00	1.50	0.46	28.17	0.12	0.04	100.21
41	Gule	A-47		30.75	36.07	0.19	0.00	0.00	0.79	0.22	27.74	0.14	0.01	95.95
42	Gule	A-24	rutile	0.00	98.91	0.00	0.13	0.00	0.21	0.02	0.00	0.05	0.00	99.31
43		A-21	ilmenite	0.00	50.22	0.00	0.05	0.64	49.65	0.43	0.05	0.07	0.00	101.11
44		A-6	magnetite	2.88	0.00	0.00	0.02	0.14	82.68	0.30	0.05	0.08	0.01	86.18
45		A-36	quartz	89.99	0.10	1.59	0.06	0.00	0.81	1.38	0.20	0.11	0.24	94.48
46		A-4		102.58	0.00	0.00	0.03	0.00	0.00	0.03	0.01	0.00	0.00	102.65
47	Poiskovy	A-48	K-feldspar	63.85	0.02	18.40	0.00	0.00	0.37	0.08	0.03	0.29	17.64	100.69
48	Gule	A-11	chlorite	34.71	0.28	8.68	0.30	0.16	12.68	9.10	0.70	0.26	0.85	67.79
49		A-15		37.90	0.25	11.82	0.17	0.06	26.13	2.17	1.72	0.44	0.77	81.44
50		A-15		41.00	0.12	7.27	0.03	0.05	39.20	3.10	1.27	0.45	0.50	92.98
51		A-15		43.12	0.10	12.27	0.11	0.02	30.93	2.11	1.57	0.23	0.72	91.18
52		A-15		43.60	0.08	6.28	0.06	0.02	39.32	2.99	0.85	0.51	0.38	94.09
53		A-17		30.43	0.08	12.84	0.02	0.31	22.34	17.44	0.50	0.16	0.26	84.37
54	Ingaringda	A-61		37.52	0.35	6.43	0.12	0.07	34.73	8.33	0.39	0.05	0.86	80.83
55	Maimecha	A-39		39.40	0.11	9.63	0.05	0.06	10.99	2.14	0.70	0.16	0.67	83.11
56	Gule	A-35	clayey mineral	43.54	1.46	31.95	0.13	0.07	4.39	0.21	0.63	0.02	0.10	82.50
57	Dunitovy	A-46	kaolinite	50.81	0.07	44.80	0.16	0.00	0.28	0.09	0.07	0.03	0.34	96.71

Thus, the mineral assemblage found in the stream sediments corresponds to the three phases of magmatism (Table 1). Forsterite and chromite are typical minerals of ultramafic rocks. Diopside, Fe-rich olivine, micas, ilmenite, magnetite and titanite are typomorphic for mafic and alkaline rocks. We think that aegirine, aegirine-augite and arfvedsonite were formed as a result of alkaline metasomatism under the impact on ultramafite minerals as a result of emanation of the alkaline melts, which are parent to the ijolite–carbonatite rock association. Fluids assisted in mobilization of the platinum group elements and their accumulation in apical parts of the ultramafic complexes.

Intergrowths of rock-forming minerals with native gold found in the concentrate are represented by the following groups:

1. Native Au ± forsterite ± augite-diopside ± chlorite (mineral association in the rocks of the first phase of the Guli volcano-pluton) (Tables 1 and 5).
2. Native Au + augite-diopside + diopside + orthoclase ± kaolinite (minerals paragenesis in the rocks of the third phase of intrusions).
3. Native Au ± aegirine-augite ± aegirine ± arfvedsonite ± albite ± titanite (typical associations in the rocks of the fourth phase of the intrusion).
4. Native Au + aegirine + nepheline (typical association in the rocks of the fifth intrusive phase).
5. Native Au ± melanite ± rutile ± chlorite ± kaolinite (mineral associations in the rocks of the seventh phase of the intrusion and low-temperature metasomatites).

Therefore, entrapped minerals of all magmatism phases, except for rock-forming minerals of the second phase, are present in native gold. Dark-colored minerals abruptly prevail as inclusions in native gold. Mineral associations of nepheline rocks and carbonatites playing a predominant role in the coarse gold formation are most widely developed. Typical metasomatic minerals (chlorite, kaolinite, garnets, chemically pure magnetite and feldspars) are present in the form of inclusions in all observed mineral associations. Formation of coarse native gold evidently occurred at the stage of metasomatic transformation of magmatic rocks.

3.3. Noble Metal Mineralization of the Kresty Intrusion

The Kresty massif is located 54 km southwest from the Guli Pluton. The intrusion has an ellipsoidal shape. Its northern part is overlapped by Quaternary sediments of the Yenisei-Khatanga piedmont depression (Figure 1b).

The central part is represented by dunites, wehrlites, clinopyroxenites and their ore varieties, containing perovskite and Ti-magnetite about 30–40% in volume. In the western and eastern peripheral parts of the massif, melilite rocks have developed (Figure 10).

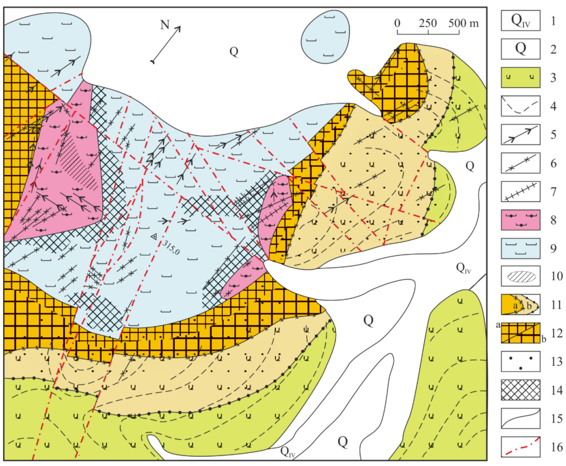

Figure 10. Map of the geological structure of the Kresty volcano–plutonic structure [1]: (1) recent alluvial sediments; (2) Quaternary sediments; (3) effusive melanephelinite stratum; (4) melanephelinite clastic lavas; (5,6) dikes: (5) alkaline microsyenites, and (6) trachybasalts, trachidolerites, plagioclase porphyrites and picrites; (7) dikes (microsyenites, trachybasalts, alkaline picrites); (8) melilitolites, also skarned; (9) olivinites, wehrlites and pyroxenites; (10) monticellitolites; (11) facies of fenites and fenitized rocks: (a) perovskite-aegirine-augite (inner and intermediate zones); outer boundary of the facies—perovskite isograde; (b) titanite-biotite-aegirine-augite (outer zone of fenitized rocks); outer boundary—titanite isograde; (12) perovskite fenites: (a) uniformly fine-grained (inner zone), (b) blastoporphyry (intermediate zone); (13) biotite-containing fenitized rocks; (14) injected melilitolite-ultramafites, skarned and recrystallized rocks of the contact zone of melilitolite bodies; (15) geological boundaries; (16) assumed faults.

Rock photographs under a microscope are provided (Figure 11).

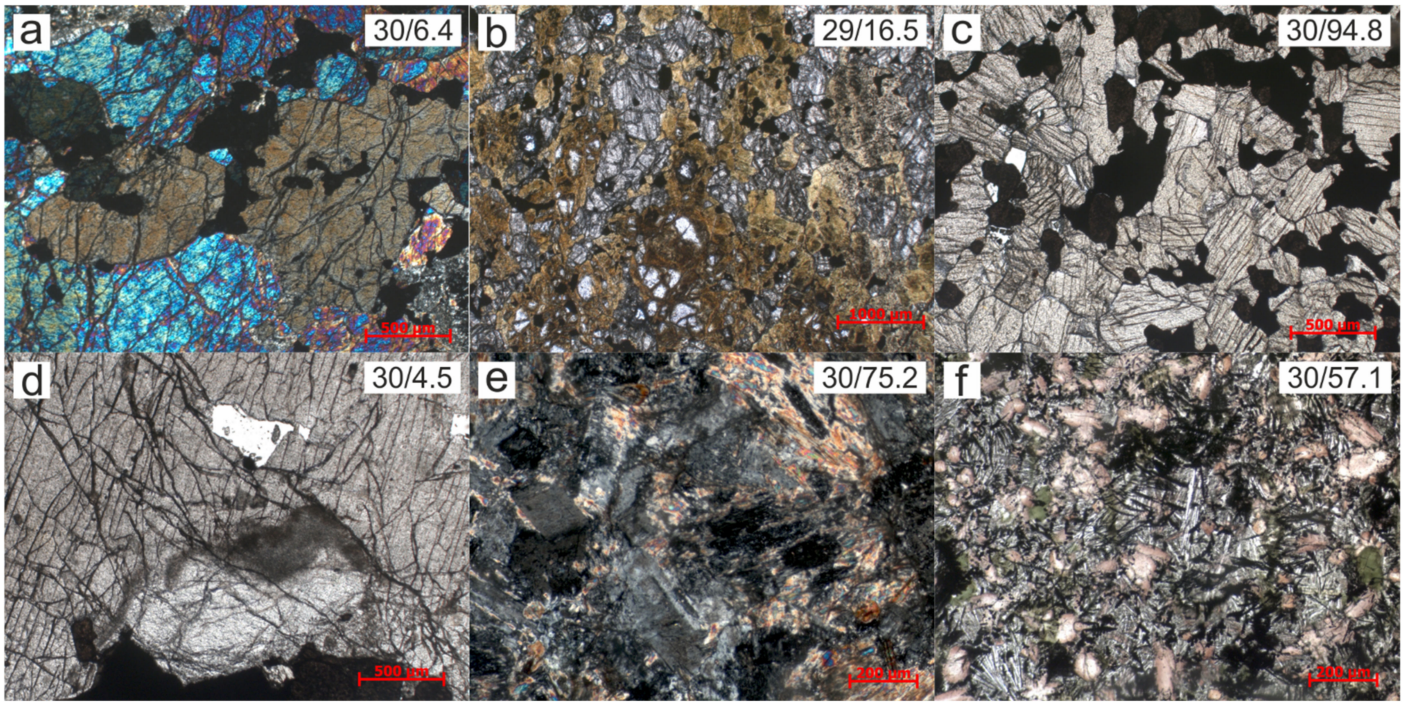

Figure 11. Rock photographs taken by microscope: (**a**) olivinites (nicols crossed); (**b**)—banded wehrlite (parallel nicols); (**c**) ore pyroxenites (parallel nicols); (**d**) kugdite (parallel nicols); (**e**) nordmarkite (nicols crossed); (**f**) alkaline picrite (parallel nicols).

Dike bodies of alkaline picrites, trachydolerites, alkaline microsyenites, microgranosyenites, calcite carbonatites and nepheline-melilite lamprophyres are distributed within the intrusion and the hosting effusive stratum. The hosting stratum is represented by predominantly melanephelinites (augitites), as well as subordinated lava flows of melilite- and leucite-containing varieties of melanephelinites and their clastic lavas.

Kugdite ages were determined on perovskite grains—249 ± 3.4 Ma. The ages of the alkaline syenites determined on accessory zircon grains—252 ± 1.0 Ma [22]. The Sm/Nd isochrone line was obtained only for the whole rock compositions of olivinites, wherlites and two pyroxenites, yielding an age of 251 ± 20 Ma ($\varepsilon_{Nd}(T)$ = +2.0). Alkaline ultramafic rocks show higher primary $^{143}Nd/^{144}Nd$ ratios ($\varepsilon_{Nd}(T)$ = +2.4 ÷ 3.1), whereas decreased values of this parameter (from −0.6 to −15.9).

Augitites located up to 1 km away from the intrusive contact suffer fenitization in the host stratum. Three zones of melanocratic fenites are identified distinctly: internal (small-grained perovskite-aegirine-augitic), intermediate (blastoporphyry perovskite-aegirine-augitic) and external (titanite-biotite-aegirine-augite fenitized augitites).

Injection melilitolites-ultramafites, recrystallized olivinites and, frequently, melilite-bearing, monticellites skarns and skarned peridotites, are formed due to the formation of melilite bodies in hosting ultramafites. Anenburg and Mavrogenes [23] and Giebel et al. [24] recommend using the term antiskarns for the skarn-like assemblage formed by fluids from alkaline rocks and carbonatites. There is essentially always a fragmentary autoreaction skarn mineralization in melilitolites. Aggregates of micro-granular inclusions of monticellite, andradite, diopside, wollastonite, vesuvianite, phlogopite, pectolite, rankinite and larnite are confined to fractures and melilitolite grain borders. Inclusions of arsenopyrite, syngenetic iron, nickel, copper and lead sulfides, native gold and platinum-group minerals are found in lower quantities together with skarn-associated minerals.

Secondary gold, platinum and palladium halos were identified on the basis of the results of prospecting geochemical work in the fields of development of fenites, fenitized rocks

and skarned ultramafites. Gold halos were identified in the field of development of monticellites. The correlation exists only between the platinum and palladium concentrations.

Platinum minerals represented by native platinum (Pt > 80%), ferriferous and isoferroplatinum of cubic symmetry and anisotropic tetraferroplatinum have been identified in crushed samples of the rocks of the Kresty intrusion. The shape of the grains is xenomorphic, with no straight boundaries. They form aggregates with perovskite, Ti-magnetite and barren rock-forming minerals. Inclusions of graphite, chalcopyrite and pyrrhotite are observed in some large grains of platinum minerals. The composition of the ferroplatinum is as follows (wt. %): Fe—11.56–11.66; Ni—0.35–0.36; Cu—0.56–0.57; Pt—81.44–83.78; Pd—0.40; and S—0.06. Refractory PGM are represented by iridium with osmium (47.59 and 29.35 wt. %), ruthenium (12.64 and 3.47 wt. %) and ir-osmium. They were found in samples from clinopyroxenites and melilitolites bodies among the aggregate of rock-forming minerals saturated with bitumen. Grains of native iridium in aggregates with Ti-magnetite and as inclusions in it were noted.

During the EPMA study of the composition of ore minerals and the presence of platinum-group elements was noted in titanomagnetite (Pt), picroilmenite (Pt), magnetite (Pt), pyrrhotite (Ir), galena (Ir, Pt, Rh, Os) and djerfisherite (Ir, Pt). PGE in oxides and sulfides are associated probably with submicroscopic inclusions of the platinum-group minerals because their distribution in the minerals is extremely irregular.

Common microscopic associations of pyrite, arsenopyrite, sphalerite, galena, bornite, boulangerite, cinnabar, native gold, cuproaurite, osmium, graphite and bitumen are developed in low-temperature hydrothermal metasomatites together with serpentine, carbonates, juanite and cebollite.

In the rocks of the Kresty intrusion, native gold occurs more frequently than other minerals of noble metals. Gold particles are commonly located in aggregates of post-magmatic silicates and in perovskite fractures, not associated with sulfides. Aggregates with sulfides are not typical for native gold, but single inclusions of gold particles in pyrite and pyrrhotite are noted. In areas where native gold particles occur, brown carbonaceous matter and graphite are noted. In the process of the EPMA analysis of Os-Ir-Rt minerals, pyrite and chalcocite grains, the presence of gold probably associated with submicroscopic inclusions of native gold in them is detected. According to the chemical composition, the following mineral varieties are identified: medium-fineness—81.9–83.6%, with copper impurity (2.96–4.64 wt. %); medium-fineness—83.6–86.2%, with insignificant mercury impurity (0.2 wt. %) and without copper impurity, extremely high-fineness—96.3–99.6%, with mercury impurity (0.13–0.88 wt. %); extremely high-fineness—97.3–98.4%, without mercury, with copper impurity (0.1–0.7 wt. %); and low-fineness—65.6%, without copper and mercury impurity—76.4%, with the mercury content up to 0.4 wt. %.

Therefore, it is worth noting that the precious-metal mineralization is confined to spot-fracture segregations of bitumen (light, oily, resinous and asphaltene), in which there are micron flakes of graphite. The following have been determined in chloroform extracts from militolites of the Kresty massif (ppm): Pt—35.3; Pd—24.3; Au—132.4; Ag—176.6; Pb—1434.8; and Cu—1438.0. The confinement of sulfides and minerals of precious metals to bitumen segregations explains the high efficiency of obtaining precious metal concentrates by adhesive oil flotation [1].

4. Discussion

4.1. Ore-Generating Magmas

It is assumed that magmas born in the mantle served as an ore substance supplier. Komatiite-meimechite and high-calcium melilite magmas and their differentiates took part in the formation of intrusions in the Maimecha-Kotuy region. Generation of such magmas occurs at different depths and at varying degrees of melting of the mantle substratum and the fluid flow conditions. According to Sobolev et al. [25–27], the melt, from which meimechites were formed, represents a primitive magma of alkaline-komatiite composition similar in the thermodynamic parameters to the Archaean analog, but with a higher content

of titanium and alkalis. Its formation is possible at partial melting of garnet peridotite. A melt separated from restite at a depth of 230–300 km at the temperature of 1640 °C as a result of diapirism of the mantle. Its primitive composition is assumed on the basis of the composition of melt inclusions in olivine from meimechite of the Guli volcano-pluton (in wt. %): SiO_2 40.81; TiO_2 2.96; Al_2O_3 3.92; FeO 12.98; MgO 28.29; CaO 6.98; Na_2O 1.23; K_2O 1.26; and P_2O_5 0.20. The primary meimechite melt was probably rich in CO_2 (5.8 wt. %) and H_2O (1.8 wt. %) in depth conditions. A high content of alkalis in the melts entrapped by olivine testifies to their systematic removal from the rocks at later magmatic and postmagmatic stages. The evolution of such magma leads to formation of ultramafic, mafic with increased alkalinity and feldspathoid syenites.

The high calcium melilite magma cannot be a differentiate of the meimechite melt. Its melting is possible at deeper levels of the mantle as compared to the meimechite melt. The melt microinclusions in melilite rock minerals correspond in terms of the composition to the approximate composition of similar alkaline magma (in wt. %): SiO_2 36.5; TiO_2 12.6; Al_2O_3 11.1; FeO 6.7; MgO 3.8; CaO 15.0; $Na_2O + K_2O$ 9.2; P_2O_5 1.5; and CO_2 3.6 [10,28–31]. It was found out that during perovskite, melilite and monticellite crystallization (1280–1160 °C) the melt suffered repeated stratification into silicate and carbonate fluids in hypabyssal magmatic chambers. The latter liquated repeatedly in the temperature range of 1200–800–600 °C with the formation of alkaline-sulfate, alkaline-phosphate, alkaline-fluoride and alkaline-chlorite salt solution melts [1,29]. They are commonly mixed with preservation of their original composition only in case of quick eruption and hardening.

4.2. Conditions of Formation and Age of the Precious Metal Mineralization

The mineralogical studies show that the Os-Ir minerals crystallized in the form of minor particles and were entrapped by olivine and chromian spinel of the meimechite melt. It is assumed that the residual refractory PGM in the depleted mantle substratum were present as very fine particles of metallic alloys. Magma chamber formation of more primitive magma was accompanied by the growth of particles of refractory PGM up to the formation of nuggets. Meanwhile, interstitial solutions circulating in the intergranular medium assisted in the growth of osmium and iridium particles. The lower temperature limit of generation of the metallic alloy saturated with PGEs from the meimechite magma is at least 1070 °C [32].

The studies of the isotope system ^{187}Os-^{188}Os [7–9] showed that the reference age of the ruthenium-iridium-osmium mineralization in the Central block of the Guli Massif is in the interval of 545–615 Ma, and a more ancient reference dating (745–760 Ma) is typical for its southwestern fragment. Our data on the basis of the Sm–Nd reconstruction of the reference age for the Kresty Massif, taking into account the probable variation in such characteristics for a series of alkaline intrusions of the province, supports these data (Figure 12).

The melilite and monticellite rocks of this unit, which are most similar to the primary mantle source, are characterized by the T_{DM} values in the range of 580–700 Ma [22]. This time interval corresponds quite well to the age of formation of the lithosphere mantle in the Paleo Asian Ocean and allows for the interaction of such a substratum with the material of the Siberian superplume [10,33–35]. A significant variety of the rock composition of the intrusions under study (Table 1, Figure 2) testifies to heterogeneous oxidation and a high degree of oxidation of mantel fluids in the zone of magma generation, which is indicated by [32,33,35,36].

The observed variations in the model values of the age as per the Os system testify to the heterogeneity of the intrusion blocks and centers of magma generation of the Guli pluton. Meanwhile, significant heterogeneity in the chemical composition is noted in the structure of the grains of Os-Ir-Ru minerals. It is probably associated with the duration of their formation, i.e., additional growth and re-crystallization of minor grains to larger ones at alternating values of fO_2. The age of formation of the Guli intrusion, estimated to be 251 ± 2 Ma [1,17,37], probably means removal by intruding melts of very fine individuals

of the Ru-Ir-Os mineralization formed at significantly earlier episodes of magma generation of the mantel substratum in the interval of 765–545 Ma.

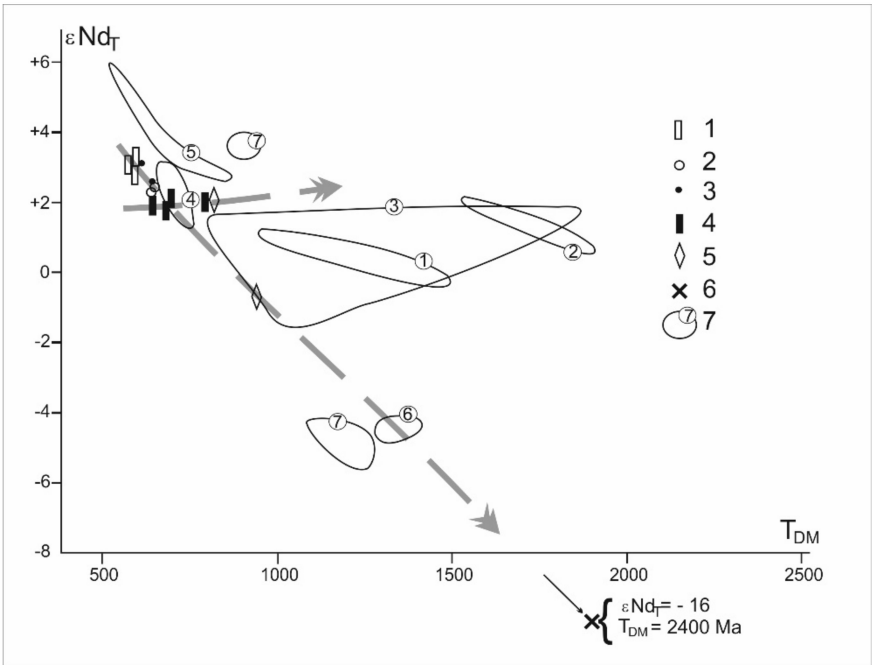

Figure 12. Sm–Nd reconstruction of the age for the Kresty Massif of the Kresty volcano–plutonic structure rocks, composition fields of volcanic and intrusive complexes of the Maimecha-Kotuy alkaline province and Taymyr lamproites on the εNd_T–T_{DM} diagram: (1) monticellitolites; (2) melilitolites and melilite-bearing olivinites; (3) melanephelinites; (4) olivinites, wehrlites and clinopyroxenites; (5) trachydolerites and trachyandesites; (6) alkaline syenite. (7) variation fields are shown with thin lines: ① volcanites of the Pravoboyarskaya suite; ② rocks of the Onchukanskaya suite; ③ alkaline effusives of the Tyvankitskaya suite; ④ nephelinites of the Delkanskaya suite; ⑤ picrites of the Maimecha suite; ⑥ lamproites of the Taimyr peninsula; ⑦ lamproites of the Chyia complex (Gorny Altai region, Southern Siberia).

Studies of silicate inclusions in PGM are of great importance in interpreting the conditions of its formation [38–40]. Nixon et al. [41] concluded that PGE mineralization in lode and placer deposits associated with the Tulameen complex (British Columbia) were formed from silicate magmatic melt during chromite deposition. They believe that silicate inclusions in PGM nuggets (clinopyroxene, magnesian flogopite, biotite, hornblende, plagioclase, sericite, chlorite and epidote) were formed during the metamorphism of the greenschist facies of ore-bearing rocks. Johan [39], based on the associations of minerals in inclusions in PGM from the placers of Nizhny Tagil (Middle Urals), came to the conclusion that ore mineralization was formed in two stages—at high and low pressures and temperatures from 1100 to 700 °C. Peck et al. [40], based on the study of mineral inclusions in PGM, concluded that the Os-Ir-Ru alloys from the placers of western Tasmania are spatially related to the basite-ultrabasic complexes. PGM are confined to the dunites. Moreover, PGM crystallized before magmatic melts appeared in crustal magma chambers.

Experimental studies [42] on the behavior of noble metal nanoparticles and Fe-Ti and PGE oxides in silicate melts showed that during slow melt cooling dispersed PGM particles are enlarged. Crystallization of Fe and Cr oxides causes formation of a redox gradient in the silicate melt in oxide-rich zones and the PGM crystallization in these areas [43]. The presence of entrapped minerals, such as augite, aegirine, magnetite and ilmenite in osmium nuggets indicates a locally non-uniform redox environment for their growth. Markl et al. [43] showed that oxygen fugacity is controlled by the potassium/sodium content in the fluid. In our case, heterogeneity of the redox environment of osmium

crystallization is confirmed by the presence of the potassium mineral phlogopite-biotite and sodium mineral aegirine in it. The presence of entrapped minerals (augite-diopside, phlogopite, aegirine, magnetite and ilmenite) in nugget Os-Ir-Ru mineral formations testifies to the long-term process of their growth. The presence of inclusions of rock-forming minerals from the 4th and 5th magmatic phases in the overwhelming majority of osmium grains, in addition to the 1st phase minerals, indicates the long-term re-crystallization of Os-Ir-Ru minerals in the process of both differentiation of the basic ultramafic magma and at the metasomatism stage. This is confirmed by the fact that the areas of concentration of the ruthenium-iridium-osmium mineralization are located in contact zones of magmatites of phases heterogeneous in time.

The role of other platinoids in the ore mineral formation of the 1st phase is abruptly subordinated. The thermal properties of the Pt + Pd + Rh and Ag + Au associations lead to their segregation in the lower temperature field of magmatogenic-hydrothermal melts. The level of affinity with the iron as well as hydrogen, oxygen and sulfur determines the accumulation of the Pt + Pd + Rh triad in later differentiates of magmatic melts. Increased platinum concentrations were noted in magnetite-bearing pyroxenites, peridotites, magnetitolites and magnetite-melilite antiskarns. Palladium is concentrated in anomalous values in nepheline rocks and carbonatites. He et al. [44] concluded that sulfides enriched in PGE are converted to sulfate in carbonate melts of the mantle with the release of PGE into the carbonate melt. In our case, carbonatites contain elevated concentrations of palladium, gold and silver (Table 2). Platinum, palladium and rhodium partially form osmium and are concentrated in sulfides, and isoferroplatinum is formed in favorable conditions. Palladium and platinum minerals are found in insignificant quantities in aggregates and inclusions in osmium. Minor inclusions of platinum and palladium sulfides, arsenides, antimonides and tellurides are explained by an abruptly subordinated quantity of sulfur, arsenic, antimony and tellurium in the ore forming system. Anenburg et al. [37] suggest that PGM nanoparticles can be transported by silicate melts from places of origin without concentration by sulfide fluids.

Gold and silver in anomalous concentrations are found in meimechites, dunites, titanium-magnetite peridotites and pyroxenites, magnetitolites, melilite rocks, ijolites, urtites and carbonatites. It is worth noting that, in this case, the rocks contain sulfides, commonly in very minor quantities. The inclusions of rock-forming minerals of all magmatism phases in native gold indicate the participation in the gold ore process of meimechite, melilite, foidite and carbonatite melts in the wide range of mineral deposition temperatures. Enlargement of native gold particles and continuing deposition of gold and silver minerals occurred at temperatures of 415–200 °C at the metasomatic stage [1,11,12]. This is confirmed by the presence of inclusions in gold-bearing minerals of metasomatic paragenesis (rutile, magnetite, diopside, garnets, chlorite, etc.). The upper temperature limit of the postmagmatic ore formation was defined on the basis of the temperature of the stable cuproaurite phase formation. The lower border of the gold-bearing minerals deposition is less definite, and corresponds to the temperature of hydrothermal metasomatism with the formation of gold parageneses with kaolinite. The variety of native gold in terms of fineness classes and the presence of electrum, küstelite and cuproaurite are associated with the heterogeneity of crystallization conditions in the area of shallow depths at the front of mixing of reduced and oxidated fluids. A high concentration (more than 60%) of large native gold particles in placers testifies to the predominance of coarse mineral particles in primary ores formed from the solutions highly saturated with gold, which existed for a long time in the ore formation system.

5. Conclusions

We presented new data on the relationship between PGM formation and multiphase alkaline-ultrabasic and melilitholite-carbonatite magmatism of the Maimecha-Kotui province. Silicate inclusions were found in native gold and Os-Ir-Ru minerals from placers within the Guli intrusion. Mineral associations of these inclusions correspond to parage-

neses of ultramafites, foidolites, alkaline gabbroids, syenites, melilitolites and foskorite-carbonatite derivatives. This can testify to the immediate participation of differentiates of the komatiite-meimechite, melilitite and carbonatite magmas in the formation of the Au-PGM mineralization. The precious metal mineralization in magmatic rocks accumulated in the oily-resinous-asphaltene bitumen of spot-fracture distribution.

Therefore, the massifs of alkaline-ultramafic rocks and carbonatites of the Maimecha-Kotuy Province are potential units for discovering a localized hardrock precious-metal mineralization associated genetically with primary meimechite and high-calcium alkaline (melilitite) magmas and their differentiates.

Close association of native gold and platinum metal minerals with carbonaceous segregations in the rocks testifies to a wide participation of hydrocarbons in the transmission, deposition and accumulation of gold and PGE. This allowed us to identify the carbonaceous-gold-platinum ore formation related to the ultramafic, alkaline and carbonatite magmatism of the central type, widening the idea on the genesis of precious metals and the prospecting area [2,13,45].

Author Contributions: Conceptual idea, the basic text, methodology and interpretation of geological and analytic data, A.M.S.; interpretation of geochemical and isotopic data, I.F.G.; diagnostics of ore minerals and estimation of rare and precious minerals, A.E.R., S.A.S. and E.A.Z.; total estimation of tectonic setting and some sample collection, O.M.G.; petrographic and mineralogical interpretation of basic rocks, T.S.K.; reconstruction of massive forms according to geophysical data, Y.V.K. All authors have read and agreed to the published version of the manuscript.

Funding: Geological and survey field studies were financed by the Norilsk Exploration Expedition. The studies were completed on the basis of the grant in accordance with Resolution of the RF Government (Agreement No. 14.Y26.31.0012). Measurements of the concentrations of precious metals in the rocks of the Guli Intrusion were funded by the State Assignment of the Ministry of Science and Higher Education of the Russian Federation (Project No. 0721-2020-0041). Determination of composition of minerals of platinum metals and gold from placers of the Gulinskaya area were funded by RFBR, Krasnoyarsk Territory and Krasnoyarsk Regional Fund of Science, project number 20-45-243001.

Acknowledgments: We are grateful to Reviewers and the Editorial Board members, for their comments and improvements.

Conflicts of Interest: The authors declare no conflict of interest.

References

1. Sazonov, A.M.; Zvyagina, E.A.; Leontyev, S.I.; Gertner, I.F.; Krasnova, T.S.; Kolmakov, Y.V.; Panina, L.I.; Chernyshov, A.I.; Makeyev, S. *Platinum-Bearing Alkaline-Ultramafic Intrusions of Polar Siberia*; CNTI Publishing House: Tomsk, Russia, 2001; pp. 1–510. (In Russian)
2. Dodin, D.A. *Metallogeny of the Taymyr-Norilsk Region (North of Central Siberia)*; Nauka: Saint Petersburg, Russia, 2002; pp. 1–822. (In Russian)
3. Kogarko, L.N.; Ukhanov, A.V.; Nikolskaya, N.E. New data on the content of platinum group elements in the rocks of the ijolite-carbonatite formation (Guli and Kugda massifs, Maimecha-Kotuy province, Polar Siberia). *Geochemistry* **1994**, *11*, 1568–1577. (In Russian)
4. Lazarenko, V.G.; Malich, K.N.; Lopatin, G.G. Geochemistry of ultramafites of the platinum-bearing Guli massif in the Maimecha-Kotuy province. *Geochemistry* **1993**, *11*, 1523–1532. (In Russian)
5. Malich, K.N.; Malich, N.S.; Simonov, O.N.; Lopatin, G.G.; Naumenko, N.G. Iridium-osmium placers of the Maimecha-Kotuy province—The new Russian source for refractory platinoids. *Nativ. Geol.* **1998**, *3*, 30–34. (In Russian)
6. Malich, K.N.; Ozhe, T. Composition of inclusions in osmium minerals—The indicator of conditions of the Guli ultramafic massif formation. *Dokl. Earth Sci.* **1998**, *361*, 812–815. (In Russian)
7. Malich, K.N. Morphology, chemical composition and osmium-isotope systematics of osmium minerals in the Guli massif (Maimecha-Kotuy province, Siberian platform). *Taymyr Nat. Resour.* **2004**, *2*, 258–276.
8. Malitch, K.N.; Badanina, I.Y.; Kostoyanov, A.I. Initial Os-isotopic composition of Os-Ir-Ru alloys from ultramafic massifs of the Polar Siberia. *Dokl. Earth Sci.* **2011**, *440*, 1343. [CrossRef]
9. Malitch, K.N.; Sorokhtina, N.V.; Badanina, I.Y.; Kononkova, N.N. Parent sources of noble-metal placers of the Guli Massif (Polar Siberia): New mineralogical data. *Dokl. Earth Sci.* **2013**, *451*, 743–745. [CrossRef]

10. Ryabchikov, I.D.; Kogarko, L.N. Oxygen potential and geochemistry of platinoids in ultramafic—Alkaline complexes. *Geol. Ore Depos.* **2012**, *54*, 291–304. [CrossRef]
11. Ryabchikov, I.D.; Kogarko, L.N.; Sazonov, A.M.; Kononkova, N.N. Formation of gold mineralization in ultramafic alkalic magmatic complexes. *Dokl. Earth Sci.* **2016**, *468*, 623–625. [CrossRef]
12. Sazonov, A.M.; Romanovsky, A.E.; Grinev, O.M.; Mayorova, O.N.; Pospelova, L.N. Precious-metal mineralization of the Guli intrusion. *Russ. Geol. Geophys.* **1994**, *9*, 51–65. (In Russian)
13. Nekrasov, I.Y. *Geochemistry, Mineralogy and Genesis of Gold-Ore Deposits*; Nauka: Moscow, Russia, 1991; pp. 1–304. (In Russian)
14. Egorov, L.S. *Ijolite-Carbonatite Plutonism*; Nedra: Leningrad, Russia, 1991; pp. 1–260. (In Russian)
15. Simonov, V.A.; Vasil'ev, Y.R.; Stupakov, S.I.; Kotlyarov, A.V.; Karmanov, N.S. Petrogenesis of dunites of the Guli ultrabasic massif (northern Siberian Platform). *Russ. Geol. Geophys.* **2016**, *57*, 1696–1715. [CrossRef]
16. Dalrymple, G.B.; Czamanske, G.K.; Fedorenko, V.A.; Simonov, O.N.; Lanphere, M.A.; Likhachev, A.P. A reconnaissance Ar^{40}/Ar^{39} geochronological study of ore-bearing and related rocks, Siberian Russia. *Geochim. Cosmochim. Acta* **1995**, *59*, 2071–2083. [CrossRef]
17. Kamo, S.L.; Gerald, K.; Czamanske, G.K.; Amelin, Y.; Fedorenko, V.A.; Davis, D.W.; Trofimov, V.R. Rapid eruption of Siberian flood-volcanic rocks and evidence for coincidence with the Permian–Triassic boundary and mass extinction at 251 Ma. *Earth Planet. Sci. Lett.* **2003**, *214*, 75–91. [CrossRef]
18. Basu, A.R.; Poreda, R.J.; Teichmann, F.; Vasiliev, Y.R.; Sobolev, N.V.; Turin, B.D. High-^{3}He plume origin and temporal-spatial evolution of the Siberian flood basalts. *Science* **1995**, *269*, 822–825. [CrossRef]
19. Kogarko, L.N.; Zartman, R.E. New data on the age of the Guli intrusion and implications for the relationships between alkaline magmatism in the Maymecha-Kotuy province and the Siberian superplume: U-Th-Pb isotopic systematics. *Geochem. Int.* **2011**, *49*, 439–448. [CrossRef]
20. Burgess, S.D.; Bowring, S.A. High-precision geochronology confirms voluminous magmatism before, during, and after Earth's most severe extinction. *Sci. Adv.* **2015**, *1*, e1500470. [CrossRef] [PubMed]
21. Palme, H.; O'Neill, H.S.C. *Cosmochemical Estimates of Mantle Composition, in Treatise on Geochemistry*; Holland, H.D., Turekian, K.K., Eds.; Elsevier: New York, NY, USA, 2003; Volume 2, pp. 1–38. [CrossRef]
22. Sazonov, A.M.; Zvyagina, E.A.; Gertner, I.F.; Krasnova, T.S.; Lipenkov, G.P. Specifics of geological composition, geochemistry and geochronology of rocks from the Kresty alkaline-ultrabasic massif (Maimecha-Kotui province, Polar Siberia). *IOP Conf. Ser. Earth Environ. Sci.* **2017**, *110*, 012006. [CrossRef]
23. Anenburg, M.; Mavrogenes, J.A. Carbonatitic versus hydrothermal origin for fluorapatite REE-Th deposits: Experimental study of REE transport and crustal "antiskarn" metasomatism. *Am. J. Sci.* **2018**, *318*, 335–366. [CrossRef]
24. Giebel, R.J.; Parsapoor, A.; Walter, B.F.; Braunger, S.; Marks, M.A.W.; Wenzel, T.; Markl, G. Evidence for magma—Wall rock interaction in carbonatites from the Kaiserstuhl Volcanic Complex (Southwest Germany). *J. Petrol.* **2019**, *60*, 1163–1194. [CrossRef]
25. Sobolev, A.V.; Slutsky, A.B. Composition and conditions of crystallization of the basic melt from Siberian meimechites in connection with the general problem of ultramafic magmas. *Russ. Geol. Geophys.* **1984**, *12*, 97–110. (In Russian)
26. Sobolev, A.V.; Kamenetsky, V.S.; Kononkova, N.N. New data on the petrology of Siberian meimechites. *Geochem. Int.* **1992**, *29*, 10–20.
27. Panina, L.I.; Sazonov, A.M.; Usoltseva, L.M. Melilite and melilite-containing rocks of the Kresty intrusion (Polar Siberia) and their genesis. *Russ. Geol. Geophys.* **2001**, *42*, 1314–1332. (In Russian)
28. Panina, L.I.; Motorina, I.V. Liquid incompatibility of deep magmas and origination of carbonatite melts. *Geochem. Int.* **2008**, *46*, 448–464. [CrossRef]
29. Panina, L.I.; Usoltseva, L.M. Pyroxenites of the Kresty alkaline-ultramafic intrusion: Composition of parent magmas and their sources. *Geochem. Int.* **2009**, *47*, 358–371. [CrossRef]
30. Rass, I.T.; Plechov, P.Y. Inclusions of melts in olivines of olivine-melilite rocks, Guli massif, northwest of the Siberian platform. *Dokl. Earth Sci.* **2000**, *375*, 389–392. (In Russian)
31. Rass, I.T. Melilite rocks of the alkaline-ultramafic complexes in the northwest of Siberia: Petrochemistry, geochemistry, genesis. *Geochem. Int.* **2000**, *10*, 1098–1108.
32. Elliott, H.; Wall, F.; Chakhmouradian, A.; Siegfried, P.; Dahlgren, S.; Weatherley, S.; Finch, A.; Marks, M.; Dowman, E.; Deady, E. Fenites associated with carbonatite complexes: A review. *Ore Geol. Rev.* **2018**, *93*, 38–59. [CrossRef]
33. Braunger, S.; Marks, M.A.; Wenzel, T.; Chmyz, L.; Azzone, R.G.; Markl, G. Do carbonatites and alkaline rocks reflect variable redox conditions in their upper mantle source? *Earth Planet. Sci. Lett.* **2020**, *533*, 116041. [CrossRef]
34. Ernst, R.E.; Bell, K. Large igneous provinces (LIPs) and carbonatites. *Mineral. Petrol.* **2009**, *98*, 55–76. [CrossRef]
35. Choi, E.; Fiorentini, M.L.; Hughes, H.S.; Giuliani, A. Platinum-group element and Au geochemistry of Late Archean to Proterozoic calc-alkaline and alkaline magmas in the Yilgarn Craton, Western Australia. *Lithos* **2020**, *374*, 105716. [CrossRef]
36. Gertner, I.F.; Vrublevskii, V.V.; Sazonov, A.M.; Krasnova, T.S.; Kolmakov, Y.V.; Zvyagina, E.A.; Tishin, P.A.; Voitenko, D.N. Isotope composition and magmatic sources of the Kresty volcano-pluton, Polar Siberia. *Dokl. Earth Sci.* **2009**, *427*, 1–7. [CrossRef]
37. Anenburg, M.; Mavrogenes, J.A. Experimental observations on noble metal nanonuggets and Fe-Ti oxides, and the transport of platinum group elements in silicate melts. *Geochim. Cosmochim. Acta* **2016**, *192*, 258–278. [CrossRef]
38. Kutyrev, A.; Kamenetsky, V.; Sidorov, E.; Abersteiner, A.; Chubarov, V. Silicate inclusions in isoferroplatinum: Constraints on the origin of platinum mineralization in podiform chromitites. *Ore Geol. Rev.* **2020**, *119*, 103367. [CrossRef]

39. Johan, Z. Platinum-group minerals from placers related to the Nizhni Tagil (Middle Urals, Russia) Uralian-Alaskan-type ultramafic complex: Ore-mineralogy and study of silicate inclusions in (Pt, Fe) alloys. *Mineral. Petrol.* **2006**, *87*, 1–30. [CrossRef]
40. Peck, D.C.; Keays, R.R.; Ford, R.J. Direct crystallization of refractory platinum-group element alloys from boninitic magmas: Evidence from Western Tasmania. *Aust. J. Earth Sci.* **1992**, *39*, 373–387. [CrossRef]
41. Nixon, G.T.; Cabri, L.J.; Laflamme, J.H.G. Platinum-group-element mineralization in lode and placer deposits associated with the Tulameen Alaskan-type complex, British Columbia. *Can. Mineral.* **1990**, *28*, 503–535.
42. Finnigan, C.S.; Brenan, J.M.; Mungall, J.E.; McDonough, W.F. Experiments and models bearing on the role of chromite as a collector of platinum group minerals by local reduction. *J. Petrol.* **2008**, *49*, 1647–1665. [CrossRef]
43. Markl, G.; Marks, M.A.W.; Frost, B.R. On the controls of oxygen fugacity in the generation and crystallization of peralkaline melts. *J. Petrol.* **2010**, *51*, 1831–1847. [CrossRef]
44. He, D.; Liu, Y.; Moynier, F.; Foley, S.F.; Chen, C. Platinum group element mobilization in the mantle enhanced by recycled sedimentary carbonate. *Earth Planet. Sci. Lett.* **2020**, *541*, 116262. [CrossRef]
45. Safonov, Y.G. Critical issues of the theory of gold ore deposits formation. *Geol. Ore Depos.* **2010**, *52*, 487–511. [CrossRef]